

Upgrade trigger & reconstruction strategy: 2017 milestone

J. Albrecht¹, P. Billoir⁸, D. Campora^{2,9}, M. Cattaneo², M. Chefdeville¹⁴, M. Clemencic², B. Couturier², A. Dziurda², C. Fitzpatrick³, M. Fontana^{2,4}, L. Grillo¹⁰, C. Hasse^{1,2}, D. Hill⁵, C. Jones⁶, F. Lemaître², O. Lupton², R. Matev², A. Pearce², F. Polci⁸, L. Promberger², S. Ponce², R. Quagliani⁸, G. Raven¹¹, B. Sciascia⁷, M. Schiller¹², S. Stahl², M. Szymanski¹³

¹*TU Dortmund*, ²*CERN*, ³*EPFL Lausanne*, ⁴*Cagliari*, ⁵*Oxford*, ⁶*Cambridge*, ⁷*LNF Frascati*, ⁸*LPNHE*,
⁹*Universidad de Sevilla*, ¹⁰*University of Manchester*, ¹¹*NIKHEF*, ¹²*University of Glasgow*, ¹³*University of Chinese Academy of Sciences*, ¹⁴*LAPP Annecy*

Abstract

The LHCb collaboration is currently preparing an update of the experiment to take data in Run 3 of the LHC. The dominant feature of this upgrade is a trigger-less readout of the full detector followed by a full software trigger. To make optimal use of the collected data, the events are reconstructed at the inelastic collision rate of 30 MHz. This document presents the baseline trigger and reconstruction strategy as of the end of 2017.

1	Contents	
2	1 Introduction	2
3	2 Reconstruction overview: Run II	2
4	2.1 Tracking	2
5	2.2 Particle identification	4
6	2.2.1 RICH PID	4
7	2.2.2 Muon PID	6
8	2.2.3 Calo PID	9
9	2.2.4 Global PID	11
10	3 Functional framework	12
11	4 Requirements: Event model	12
12	5 Reconstruction overview: Run III	13
13	5.1 Tracking	13
14	5.1.1 Developments since LHCb-PUB-2017-005 [20]	14
15	5.1.2 Ongoing developments	15
16	5.1.3 Future developments	16
17	5.2 Particle identification	17
18	5.2.1 RICH PID	17
19	5.2.2 Muon PID	17
20	5.2.3 Calo PID	18
21	5.2.4 Global PID	18
22	6 Trigger	18
23	6.1 Selection framework	19
24	6.1.1 HLT1 selections	20
25	6.1.2 HLT2 selections	20
26	6.1.3 Combinatorics	21
27	6.1.4 Looking forward	22
28	6.2 Persistency	23
29	6.2.1 Persistency of trigger decisions	23
30	6.2.2 Turbo persistency	23
31	6.2.3 TESLA	25
32	6.2.4 Looking forward	25
33	7 Conclusion	26
34	References	28

1 Introduction

This document presents the baseline trigger and reconstruction strategy as of the end of 2017. The reconstruction as implemented in Run 2 is presented first to set a baseline, followed by the developments that yield towards the Run 3 reconstruction sequence. Differences between Run 2 and Run 3 are emphasised and the current algorithmic implementation is given. The document is structured as follows:

Chapter 2 gives an overview of the Run 2 reconstruction. It begins with a discussion of the tracking sequence, followed by the particle identification sequence. Chapter 3 then introduces the *functional framework* in which the upgrade reconstruction algorithms are implemented. Chapter 4 gives a short overview of the requirements on the event model. Chapter 5 then discusses the Run 3 sequence, structured in tracking and PID parts. Chapter 6 then discusses the trigger strategy for Run 3, including the selection framework and persistency.

2 Reconstruction overview: Run II

2.1 Tracking

The LHCb tracking system consists of three detectors: the VELO, the TT and the T stations. Information from these detectors is used to reconstruct the following types of tracks:

- **VELO tracks**,
are made using the VELO detector and are used in finding primary vertices.
- **Upstream tracks**,
are reconstructed from VELO tracks and TT hits. These tend to be low momentum particles which are then swept out of the LHCb acceptance by the magnet.
- **T tracks**,
are determined from hits in the T stations, sometimes referred to as a **Seed tracks**.
- **Downstream tracks**,
have both TT and T station hits, but do not use the VELO detector. This type of track is important in the reconstruction of daughters from long-lived particles such as K_s^0 or Λ , which often decay after leaving the VELO detector.
- **Long (Forward, Match) tracks**,
have signatures in at least the VELO and T stations. Since these tracks pass through the magnetic field, they have the most accurately measured momentum. Depending on the reconstruction algorithm they are called either **Forward** or **Match** tracks.

Due to their properties downstream and long tracks are the most useful for physics analyses. The different types of tracks are presented in Fig. 1.

The track reconstruction consists of three main parts. First, the signatures produced by charged particles in the detector, tracks, are found by pattern recognition algorithms. Second, all of the found tracks fit using a Kalman filter which obtains the best possible estimate of the true trajectory with corrections due to energy loss and multiple scattering.

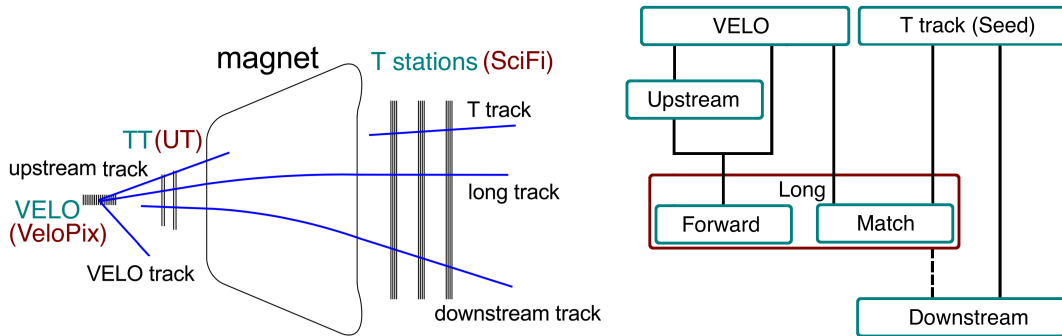


Figure 1: Left: different types of tracks in the LHCb experiment. The tracking system subdetectors are indicated in a cyan (red) for Run II (Upgrade), while the track types are shown as blue lines. Right: dependencies among the different types of tracks.

74 Finally, any particles that are reconstructed twice by different algorithms are removed
 75 and a container with the best unique tracks is created.

76 The track reconstruction currently consists of several independent algorithms. The
 77 source code of which can be found in the LHCb/Rec gitlab repository [1]. The dependencies
 78 among different type of tracks are shown in the right part of Fig. 1. Two basic algorithms
 79 are `FastVeloTracking` [2] and `PatSeeding` [3] which reconstruct the VELO and T-track
 80 candidates, respectively. Those tracks are then used as an input to other algorithms.
 81 Upstream track candidates are reconstructed from the VELO tracks and hits in the TT
 82 using dedicated `PatVeloTTHybrid` [4] algorithm. We specify two types of long tracks:
 83 forward and match. The first, reconstructed using (`PatForward{HLT1|HLT2}` [5]), starts
 84 with upstream (HLT1) or VELO (HLT2) tracks and searches for corresponding hits in
 85 the T stations. The latter, called the track matching (`PatMatch` [6, 7]), uses both VELO
 86 and T tracks as input and matches them in the magnet region. Finally, the downstream
 87 algorithm (`PatLongLivedTracking` [8]) uses T-track candidates as seeds and searches for
 88 corresponding clusters in the TT. The outputs of all algorithms are merged, eliminating
 89 candidates that were found twice. After cutting on the χ^2/ndof of the track approximately
 90 22% of all reconstructed long tracks are still estimated to be fake. To further reduce this
 91 rate, a requirement on the ghost probability [9], is used which reduces about 1/3 of fake
 92 tracks. In addition to the track finding, the tracking sequence determines primary vertices
 93 (PVs). The PV finding algorithm (`PatPV3D` [10, 11]) uses the Kalman Filtered VELO
 94 tracks to determine the position of proton-proton interactions in the event.

95 In Run II (2015-2018) the LHCb experiment introduced real-time reconstruction which
 96 unifies the online and offline processing [12]. All of the tracking algorithms have to fit
 97 in the trigger timing budget, resulting in a two step procedure. In HLT1, all VELO
 98 tracks are reconstructed and fit with a simplified Kalman filter. Then the primary vertex
 99 finding is performed. These VELO tracks serve as an input to the Upstream tracking,
 100 where an initial momentum estimate is made. Upstream tracks are subject to a transverse
 101 momentum cut, which is presently > 400 MeV/c prior to the forward tracking. After the
 102 forward tracking this is further tightened to > 500 MeV/c, and a Kalman fit is applied
 103 resulting in long tracks. These long tracks are the necessary input to the tracker alignment
 104 task. The second stage, HLT2, runs with looser requirements. Remaining VELO tracks,
 105 which were not extended into long tracks, are propagated to the T stations, this time
 106 without a transverse momentum threshold and without requiring clusters in the TT. At

107 this point, the output of both forward tracking algorithms is merged. A standalone T track
 108 reconstruction is performed, followed by the matching and downstream algorithms. All
 109 track candidates are fit using a Kalman filter and tracks that are made more than once
 110 by the different algorithms are removed. The tracking sequence runs in both the trigger
 111 (Moore) and offline (Brunel). The tracking sequence as constructed in LHCb/Brunel [13]
 112 is as follows:

```

113 #HLT1
114 RecoVELOSeq
115   FastVeloTracking           #VELO tracks finding
116 RecoTrHLT1Seq
117   TrackHLT1
118     TrackHLT1VeloTTPatSeq
119     PatVeloTTHybrid         #Upstream tracks finding
120     TrackHLT1ForwardPatHLT1S
121     PatForwardHLT1         #Long (Forward) tracks finding
122     TrackHLT1FitHLT1Seq
123     CopyVeloTracks
124     VeloOnlyInitAlg
125     ForwardHLT1FitterAlg   #Kalman Filter Forward tracks
126 RecoVertexSeq
127   PatPV3D                   #Primary Vertex reconstruction
128   PVVeloTracksCleaner
129
130 #HLT2
131 RecoTrHLT2Seq
132   TrackHLT2
133     TrackHLT2ForwardPatHLT2S
134     PatForwardHLT2         #Long (Forward) tracks finding
135     MergeForwardHLT1HLT2   #Merge both Forward findings
136     TrackHLT2SeedPatSeq
137     PatSeeding             #T-tracks finding
138     TrackHLT2MatchPatSeq
139     PatMatch               #Long (Match) tracks finding
140     TrackHLT2DownstreamPatSe
141     PatLongLivedTracking   #Downstream tracks finding
142   FitHLT2
143     FitHLT2BestSeq
144     TrackBestTrackCreator  #Kalman Filter and clone killing

```

145 2.2 Particle identification

146 2.2.1 RICH PID

147 RICH reconstruction involves a number of steps, that can broadly be broadly classified as:

- 148 1. Pixel Processing. This sequence deals with the RICH raw data. It is first decoded
 149 into unique channel identifiers. Optionally, clustering can then be performed if

150 required (not done in Run II for HPDs, but might be required with MaPMTs in
151 Run III). Finally the position of these pixels (or clusters) are computed in both
152 global and local RICH coordinate systems.

153 2. Track Processing. This sequence takes the Track objects as provided by the tracking
154 system, and computes a number of quantities from them. First, the intersections
155 with the RICH1 and RICH2 radiator volumes need to be determined. For a track to
156 be considered for processing in the RICH, it must have an intersection with at least
157 one radiator. This produces 'segments' which describe the trajectory through the
158 radiator volume. The segments are then ray traced (as if it were a photon) through
159 the RICH mirror system to the detector plane, and the hit positions are computed.
160 The photon yields, expected Cherenkov angles and an estimate of the per track
161 Cherenkov resolution are also computed under each of the deuteron, proton, kaon,
162 pion, muon and electron mass hypotheses. An important algorithm in the sequence
163 is the one which forms the Cherenkov mass cones for each segment. This involves
164 taking each segment, and for each mass hypothesis (that is above threshold) ray
165 traces a fixed number (say 100) of Cherenkov photons at the expected Cherenkov
166 angle to the detector plane. This provides critical information on the detector
167 acceptance for each segment. Due to the large number of ray tracings this involved,
168 this was the second most CPU expensive step in the whole sequence.

169 3. Photon Reconstruction. This sequence takes the pixel and segment information
170 formed in the previous sequences, and forms candidate Cherenkov photons from
171 them. This step is the most CPU intensive due in part to the large number of
172 segment and pixel combinations that need to be considered, and in part due to the
173 computation intensity of the calculations. This is the single most CPU intensive
174 step in the processing.

175 4. PID. The final sequence takes the information produced in the previous ones, and
176 forms a description of the event based on a set of assumed mass hypotheses for each
177 track, and derived from this the expected signal and background distributions in the
178 detector. This is compared to the observed data to provide an overall event likelihood
179 for the set of mass hypotheses that were assumed. These mass assignments are then
180 changed, in an iterative minimisation of the likelihood to provide the final likelihood
181 information for each track and mass hypothesis. Combined, the algorithms running
182 in this sequence are the third most CPU expensive.

183 The following output shows how the above description of the steps in the RICH
184 processing map onto the algorithms currently running as part of the RICH sequence. Note
185 that only the sequence for Long tracks is shown. Each of the three track types (Long,
186 Downstream and Upstream) have similar, but separate, sequences for steps 2, 3 and 4
187 above.

```
188 RichRecoSeq
189   RichPixels                               Step 1. Pixel processing
190     RichPixClustering
191     RichPixGlobalPoints
192     RichPixLocalPoints
```

193	RichLongReco	Step 2. Track processing
194	RichTracksLong	
195	RichTrackSegmentsLong	cd
196	RichTrackGloPointsLong	
197	RichTrackLocPointsLong	
198	RichEmittedYieldsLong	
199	RichEmittedCKAnglesLong	
200	RichMassConesLong	
201	RichDetectableYieldsLong	
202	RichGeomEffLong	
203	RichTkSegmentSellLong	
204	RichSignalYieldsLong	
205	RichSignalCKAnglesLong	
206	RichCKResolutionsLong	
207	RichPhotonsLong	Step 3. Photon Reconstruction
208	RichPhotonRecoLong	
209	RichPredPixelSignalLong	
210	RichRecSummaryLong	
211	RichPIDLong	Step 4. Likelihood Minimisation
212	RichGPIDInitLong	
213	RichPixBackgroundsIt0Long	
214	RichGPIDLikelihoodIt0Long	
215	RichPixBackgroundsIt1Long	
216	RichGPIDLikelihoodIt1Long	
217	RichGPIDWriteRichPIDsLong	

218 Each algorithm in the above list is implemented using the developing Run 3 framework.

219 2.2.2 Muon PID

220 The identification of muons in LHCb is mostly based on the Muon detector [14], which is
221 composed in Run II of five detecting stations interleaved by the calorimeters (M1, M2)
222 and filtering iron walls (M2→ M5). The readout of the muon detector is given by the OR
223 of horizontal and vertical *physical pads*, and the crossing of the two defines a *logical pad*
224 whose dimensions give the x , y pad size associated to the hit. If there is no simultaneous
225 readout, the x , y pad size is given by the whole physical dimensions of the *physical pad*.
226 In the following we will refer to the single hits given by the *physical pads* as *uncrossed*
227 *hits*, and to the *logical pads* as *crossed hits*.

228 The muon identification algorithm is a two-step procedure (the main code is
229 `MuonIDAlgLite`). The first step identifies the incoming particle as a muon if the bi-
230 nary variable `IsMuon` is set to true. The evaluation of `IsMuon` relies on the number of
231 hits found around the tracks extrapolated through the muon stations. The size of the hit
232 search windows, named FoI (Field of Interest), are parametrised accounting for the particle
233 momentum and the muon detector regions crossed (see [15] for the details). `IsMuon` is set
234 to true, when the algorithm finds a coincidence of muon stations as a function of the mo-
235 mentum. Similar to `IsMuon`, other two boolean variables are constructed: `IsMuonLoose`
236 that requires a fewer amount of hits with respect to `IsMuon` and `IsMuonTight` than
237 requires the same amount of hits as `IsMuon`, but only *crossed hits*. The algorithms used

238 to classify the muon candidates as just described, are in `CommonMuonTool` and run both
239 at the HLT1 that at the offline reconstruction levels.

240 The second step builds a muon likelihood, DLL, using the average squared distance
241 in units of pad size, between the closest hit in FoI to the track extrapolation points on
242 each station. The DLL variable is used in the global particle identification procedure to
243 be combined with the information from the other PID detectors to evaluate a combined
244 likelihood variable. In each of the bins (samples are binned in momentum and position),
245 two tests are performed that yield $P(\mu)$, the probability of the candidate being a muon,
246 and $P(\text{not } \mu)$, the probability of the candidate not being a muon. From those quantities
247 the delta log likelihood, DLL, is calculated [15].

248 It should be noted here, that due to the two-dimensional binning, many calibration
249 constants are needed. D^2 and the DLL are saved in the muon track object. In the offline
250 reconstruction, the quantities $\log(P(\mu))$ and $\log(P(\text{not } \mu))$ are stored in the muon PID
251 object. Additionally, a track fit is performed on the extrapolation using only the closest
252 hits. The resulting χ^2/ndof is also stored in the muon track object. The DLL is used in
253 the global particle identification procedure to be combined with the information from
254 the other detectors to evaluate the combined DLL variable. Furthermore, $\log(P(\mu))$ and
255 $\log(P(\text{not } \mu))$ are used as input to a Neural Network based particle identification called
256 `ProbNN`. Details on the combined particle identification can be found in Ref. [16].

257 For each muon candidate the identification algorithm evaluate another variable,
258 `NShared`, that helps to distinguish between actual and ghost tracks. The `NShared` variable
259 has a discriminating power against background, and can contribute to the reduction of
260 particle misidentification. The DLL and the `NShared` variables are evaluated for each muon
261 candidate classified as `IsMuonLoose`, by the tools `DLLMuonTool` and `NShared` respectively.
262 The last step of the muon identification algorithm is to classify as a muon track each
263 incident track that has be found to be at least `IsMuonLoose`: this is done by the tool
264 `MakeMuonTool`.

265 The `CommonMuonTool` is used since the beginning of Run II both at the HLT2 and offline
266 reconstruction level to calculate the aforementioned variables, and is used at the HLT1
267 level to calculate `IsMuon`. Additionally, there are two tools called `CommonMuonHitManger`
268 and `DeMuonDetector`, which extract the hit information from the muon raw detector
269 data. The `CommonMuonTool` offers a dedicated method for each logical step in the `IsMuon`
270 algorithm. In addition, functions offering functionality to calculate `IsMuonLoose` and
271 `IsMuonTight` are implemented. What follows is an overview of the methods which are
272 used both in the offline reconstruction by the `MuonIDAlgLite` code and in the HLT1
273 trigger by the `IsMuonTool` code. More details on the algorithm are given below.

- 274 • The `initialize` method sets up the tool. It loads additional tools and fetches the
275 constants from the database.
- 276 • `preSelection` takes a track object and returns whether the track passes the pre-
277 selection criteria. In this case it just checks if the track momentum is larger than
278 the cut value ($p > 3 \text{ GeV}/c$).
- 279 • `extrapolateTrack` takes a track object and extrapolates it through the muon
280 stations. It returns a point (x, y) for each station (at a fixed z) except M1 which is
281 not used.

- 282 • `inAcceptance` uses the output of `extrapolateTrack` in order to check whether the
283 coordinates of the extrapolated hits are within the acceptance of the muon stations.
- 284 • `hitsAndOccupancies` takes both a track and a `MuonTrackExtrapolation` container
285 as input and returns two containers: the first holds the hits that are found in the
286 muon stations within the FoI around the extrapolations, the second container holds
287 the total number of hits in each station, which is called the occupancy of the station.
288 The latter is also used to check whether a station has hits within a FoI.
- 289 • `extractCrossed` takes the hits in the muon stations as input and selects only those
290 that are crossed. Additionally, it also calculates the new occupancies considering
291 only the crossed hits.
- 292 • `isMuon` uses occupancies and the track momentum to classify it. If it obtains a
293 container of occupancies from crossed hits, it calculates `IsMuonTight` by definition.
- 294 • `isMuonLoose` also takes a container of occupancies and a track momentum and
295 calculates `IsMuonLoose`
- 296 • `foi` for a given station, region, and momentum returns the edge of the field of
297 interest.

298 In HLT1, muon lines make use of the `IsMuonTool`, which has been adjusted in
299 order to use the functionalities offered by the `CommonMuonTool`. Like every tool that is
300 used by a trigger line, it exploits a method, `tracksFromTrack`, which takes the current
301 HLT1 reconstructed track (trigger track in the following) as input and writes to an
302 output container if the `IsMuon` criterion is met. It uses the functions `preSelection`,
303 `extrapolateTrack`, `inAcceptance`, `hitsAndOccupancies`, and `isMuon` in sequence. At
304 the HLT2 the algorithm receives a collection of reconstructed tracks as input, and the
305 calculation of `IsMuon` is embedded inside a loop over the tracks, using methods in
306 `MuonIDAlgLite` algorithm (for backwards compatibility `MuonIDAlg` still exists). The
307 algorithm accepts both long and downstream tracks.

308 Two tools are introduced in order to provide additional information that is not used in
309 HLT1. Those are called `DLLMuonTool` and `MakeMuonTool`. The `DLLMuonTool` is responsible
310 for calculating the delta log likelihood (DLL) of the muon hypothesis. It loads all the
311 parameters for the hypothesis tests in different bins in momentum and region as described
312 in Ref. [15] in order to calculate $P(\mu)$ and $P(\text{not } \mu)$. Two different implementations
313 can be used via a flag: `calcMuonLL_tanhist` and `calcMuonLL_tanhist_landau`. In the
314 first case the probabilities are extracted using the reference histograms for signal and
315 background, without analytical description. In the second case $P(\mu)$ is computed as in the
316 `calcMuonLL_tanhist` implementation, while a Landau description is used for $P(\text{not } \mu)$.
317 The default method is the second one.

318 Both return the likelihood for the muon hypothesis $P(\mu)$ as well as for the background
319 hypothesis $P(\text{not } \mu)$. It also contains the squared distance of the muon track D^2 . The
320 DLL is then calculated. Additionally, the tool allows to calculate the `NShared` variable
321 via the `calcNShared` method. This variable relies on relationships between the tracks in
322 an event. The `MakeMuonTool` is intended to create a muon track once all the necessary
323 information is there, through a function called `makeMuonTrack`. If a corresponding flag is
324 set, the tool also performs a track fit in order to obtain the χ^2 of the track.

325 The MuonPID event model has been expanded to include five more quantities that are
326 not currently used in the muon ID selection. The first quantities are already defined and
327 available for use:

- 328 • **chi2Corr**: a χ_{best}^2 accounting for correlations among the hits on different stations
329 induced by multiple scattering. It is produced by the `MuonChi2MatchTool`, called
330 for each `IsMuonLoose` candidate.
- 331 • **muonMVA1**: a Boosted Decision Tree or μ BDT obtained training space residuals,
332 multiple scattering errors, *crossed/uncrossed* hit information, `NShared`, and - for the
333 first time - also the hit times. It is produced by the `MVATool` called for each `IsMuon`
334 candidate.

335 The remaining three quantities `muonMVA2`, `muonMVA3`, and `muonMVA4` are left free for future
336 developments.

337 2.2.3 Calo PID

338 The calorimeter algorithms can be grouped into two main sequences: reconstruction
339 and PID which are respectively configured by `CaloRecoConf` and `CaloPIDConf` classes.
340 The reconstruction sequence takes as input SPD/PS, ECAL and HCAL raw banks and
341 produces calorimeter hypothesis, according to the following steps:

- 342 1. Digits preparation for the reconstruction: `CaloDigits`. This is done by processing of
343 the raw data (`SpdFromRaw`, `PrsFromRaw`, `EcalZsup`, `HCALZsup`). For the ECAL
344 and HCAL, the data is zero-suppressed; this was done at an earlier stage for the PS
345 while SPD data is binary. Cell energies are then calculated using stored calibration
346 constants.
- 347 2. Reconstruction of ECAL clusters: `ClusterReco`. This uses the cellular automaton
348 algorithm which groups digits around local energy maxima called seeds (`EcalClust`).
349 The default cut on the transverse energy E_T of the cluster is 50 MeV. In a second
350 step, the cell energies are corrected for energy leakage from neighbouring showers
351 (`EcalShare`). The formed clusters are then cropped to 3×3 cell clusters centred
352 around the seeds. This cluster shape is default in Run1 and Run2, however, different
353 shapes were implemented in view of Run3 to reduce the aforementioned leakage
354 effects which will be more pronounced at higher luminosity. Finally, the covariance
355 of the cluster is calculated (`EcalCovar`).
- 356 3. Reconstruction of photons: `PhotonReco`. Clusters are classified into charged and
357 neutral based on the extrapolation of tracks to the calorimeters. The track-cluster
358 matching quality is quantified by means of a χ_γ^2 which takes into account the
359 uncertainties both on the cluster position measurement and on the track extrap-
360 olation (`CaloTrackMatch`). Photons are formed from neutral clusters with $\chi_\gamma^2 \geq 4$
361 and $E_T \geq 200$ MeV, to which SPD/PS digits are added. The photon energy is
362 then calculated from the digit energies using Monte Carlo coefficients to correct for
363 lateral and longitudinal leakage (so-called E -corrections). The three-dimensional
364 shower barycentre is calculated from the energy-weighted 2D cluster barycentre

365 (corrected for a cell-size-dependent bias, S -corrections) and a Monte Carlo parame-
 366 terisation of the shower penetration depth with energy (L -corrections). These cuts
 367 and calculations are performed by the `SinglePhotonRec` algorithm.

- 368 4. Reconstruction of electrons: `ElectronReco`. This proceeds in a similar way as for sin-
 369 gle photons but with $\chi_\gamma^2 < 25$ and specific E - S - L -corrections (`SingleElectronRec`).
- 370 5. Reconstruction of merged π^0 : `MergedPi0Reco`. This is based on so-called split-
 371 clusters which are also produced by `ClusterReco`. The algorithm consists in splitting
 372 each of the Cellular Automaton single clusters into two interleaved 3×3 subclusters
 373 built around the two main cells of the original cluster. The energy of the common cells
 374 is then shared among the two virtual subclusters. Each of the two subclusters is then
 375 reconstructed as a single photon hypothesis cluster. In particular, E, S, L -corrections
 376 are applied to the merged π^0 reconstruction (`MergedPi0Rec`).

377 The calorimeter PID splits into a charged sequence (electrons and muons PID) and
 378 a neutral sequence (photon and merged π^0 PID). The charged sequence calculates for
 379 tracks matched to a cluster, the values of $DLLe$ and $DLLmu$ as a product of the DLL
 380 from ECAL, HCAL and PS. This is done in the following steps.

- 381 1. `InCaloAcceptance`. This sequence checks that the tracks are in the acceptance of
 382 the calorimeter so next sequences can be run.
- 383 2. `CaloMatch`. Calculates the χ^2 value of the track-cluster matching. This is done using
 384 the extrapolation of the track from its direction after the magnet (`ElectronMatch`)
 385 or before the magnet (`BremMatch`). The clusters matched by the second method are
 386 brem photon candidates.
- 387 3. `CaloEnergy`. Gets the energy along the track line as measured in the SPD, PS,
 388 ECAL and HCAL (`EcalE`, `HcalE`, `SpdE`, `PrsE`). This information will be also
 389 used for PID. In particular, PS and HCAL energy will improve the separation of
 390 electrons from other charged particles (h , μ) which leave a small energy in this
 391 detector.
- 392 4. `CaloChi2`. This is where the basic ECAL estimator is constructed as a χ_e^2 of a global
 393 matching procedure. The later includes the balance between track momentum and
 394 cluster energy, and between track extrapolation and cluster position. It is run for
 395 electron candidates (`EcalChi22ID`), brem candidates (`BremChi22ID`) and clusters
 396 (`CluChi22ID`). It makes use of the quantities calculated in previous sequences.
- 397 5. `CaloDLLe`. Calculates the $DLLe$ values for each sub-detector. This uses quantities
 398 calculated in the previous sequences and template histograms stored in a database:
 399 $DLLe^{\text{ECAL}}$ uses χ_e^2 (`EcalPIDe`), $DLLe^{\text{brem}}$ uses χ_{brem}^2 (`BremPIDe`), $DLLe^{\text{HCAL}}$ uses
 400 E_{HCAL} (`HcalPIDe`) and $DLLe^{\text{PS}}$ uses E_{PS} (`PrsPIDe`).
- 401 6. `CaloDLLmu`. Similar to the previous sequence, using as input only the energy in the
 402 ECAL (`EcalPIDmu`) and the energy in the HCAL (`HcalPIDmu`).

403 The neutral PID sequence assigns a confidence level (DLL) to the neutral calorimeter
404 hypothesis using the following inputs: χ_γ^2 , E_{seed} and E_{PS} . Reference histograms of these
405 variables are available for signal and background in each ECAL section (inner, middle,
406 outer) and for converted and non-converted photons (*i.e.* with and without hits in the
407 SPD). The sequence is ran for the three neutral hypothesis: `PhotonID`, `MergedID` and
408 `PhotonFromMergedID` for single photons, merged π^0 and split-photons.

409 2.2.4 Global PID

410 The PID information obtained separately from the muon, RICH, and calorimeter systems
411 is combined to provide a single set of more powerful variables. Two different approaches
412 are used. In the first method the likelihood information produced by each sub-system is
413 simply added linearly, to form a set of combined likelihoods, $\Delta \log \mathcal{L}_{\text{comb}}(X - \pi)$, where X
414 represents either the electron, muon, kaon, proton or deuteron mass hypothesis. These
415 variables give a measure of how likely the mass hypothesis under consideration is, for any
416 given track, relative to the pion hypothesis. Along Run I a second approach has been
417 subsequently developed to improve upon the simple log likelihood variables both by taking
418 into account correlations between the detector systems and also by including additional
419 information. This is carried out using multivariate techniques, combining PID information
420 from each sub-system into a single probability value for each particle hypothesis. These
421 variables are known as `ProbNNx`, with `x` standing for electron, muon, pion, kaon, proton,
422 or ghost. Notice that since the beginning of Run II, the `ProbNN` variables were available
423 also in the trigger.

424 Detailed information about the `ProbNN` approach is available only in presentations
425 given at meetings and in the code itself. Best information can be found here ¹ for
426 Run I and here ² for Run II. For what concerns code, the main repository is the
427 `ChargedProtoANNPID` ³. The list of variables used as input for the `ProbNN` can be
428 found here `ChargedProtoANNPID/data` for each tuning and specie. This list is used at
429 runtime to list what variables are used (looking at any specific file: the first 5 lines
430 are other settings, the inputs start on line 6; lines with a `#` at the beginning are com-
431 mented out, so not used). Technically, to know how the data are extracted, the names
432 in these files can be matched by looking at the mapping between the name and a helper
433 class `ChargedProtoANNPID/src/ChargedProtoANNPIDCommonBase.icpp` and then here
434 `ChargedProtoANNPID/src/ChargedProtoANNPIDCommonBase.h` to see exactly what each
435 helper does.

436 The training of `ProbNN` variables is done using inclusive B Monte Carlo events. Actual
437 performance depends on the tuning *i.e.* the blending of MC samples used. A large
438 collection of information on the various tunes can be found by looking in this folder ⁴.
439 Several different tunings are available for both Run I and Run II. For the Run II samples,
440 only the `MC15TuneV1` and `MC12TuneV4` `ProbNN` PID variables should be used. For all
441 Run II analyses, it is recommended to use the `MC15TuneV1` `ProbNN` variables - those of
442 `MC12TuneV4` are optional. For the Run I samples, only `MC12TuneV2` and `MC12TuneV3` are

¹<https://indico.cern.ch/event/226062/contributions/475644/attachments/371741/517276/ANNPIDRetuning-Reco14-06052013.pdf>

²<https://indico.cern.ch/event/508832/contributions/2030857/attachments/1249785/1842643/ANNPID-2015TuneV1-30032016.pdf>

³<https://svnweb.cern.ch/trac/lhcb/browser/Rec/trunk/Rec/ChargedProtoANNPID/>

⁴<http://www.hep.phy.cam.ac.uk/~jonesc/lhcb/PID/ANN/>

443 accessible. V3 is not an exact “upgrade” of V2, but it adds more kinematic regions and
444 removed ghosts from the training samples. For many decays it will be better, but there
445 might be some specific cases where it is not. Different versions of `ProbNN` variables are
446 accessible e.g. through `TupleToolANNPID` for ntuples. (Default one in other code, like
447 `LoKi`, is `MC12TuneV2` for Run I and `MC15TuneV1` for Run II.)

448 **3 Functional framework**

449 To better exploit multi- and many-core architectures, the *functional framework* was
450 introduced. Its aim is to give developers general building blocks that are well defined,
451 multithreading friendly and handle the dataflow between algorithms.

452 Every algorithm has to define its inputs and outputs. That means that at initialisation
453 time of the application a static data dependency graph can be generated to, first, prevent
454 configuration errors due to wrongly defined locations and, second, to schedule algorithms
455 in the right order according to the data dependencies. Multiple or no inputs and outputs
456 are possible. To guarantee thread safety, inputs to an algorithm are declared as constant
457 and the main execution is not allowed to change the state of an algorithm⁵.

458 The RICH reconstruction was the first big part of the reconstruction to fully embrace
459 the functional framework and modern coding ideas. It was completely redesigned, removing
460 a number of design choices incompatible with the functional framework, and put into
461 production in 2017, see Section 2.2.1 for a description.

462 **4 Requirements: Event model**

463 The event model is not described in detail here, for further information see Ref [17].
464 Some details have been mentioned in the previous sections. In summary, the event model
465 comprises two aspects, transient data and persistent data. The event model should allow
466 to pass transient objects between algorithms with little overhead and allow to persist
467 the necessary information to perform analyses. Little overhead often means to create
468 smaller objects with only minimal information for the next step. Having all the necessary
469 information available gravitates towards bigger objects. Additionally, the event model
470 has to take into account the need of data structures that better match the requirements
471 placed by modern hardware to exploit parallelism (SIMD vectorisation).

472 As an example, in HLT1 where the data have to be processed at 30 MHz any overhead
473 from memory allocations quickly contributes a significant fraction to the runtime, while
474 in HLT2 the individual reconstruction algorithms are considerably slower and overhead
475 from the event model might be negligible. Ref. [17] lays out several approaches to reduce
476 the overhead from memory allocations. One example is removing the extensive use of
477 `KeyedContainers`. Very simplified, a `KeyedContainer` assigns each member a unique key
478 which can be different to the index in the container. The `KeyedContainer` is implemented
479 as a map. Adding objects to a map is considerably slower than adding objects to a vector.
480 Replacing `KeyedContainers` in between algorithms seems obvious in many cases, but

⁵Nevertheless, the use of tools inside an algorithm and having *mutable* class members can introduce data races.

481 further simplifications are likely needed. However, the current persistency heavily relies
 482 on the use of keyed objects, *e.g.* see Section 6.2.2, and needs to be adapted.

483 5 Reconstruction overview: Run III

484 5.1 Tracking

485 The upgrade tracking sequence is designed to take an advantage of the successful Run
 486 II strategy. Two separated stages are constructed: `fast` and `best`. The first fast stage
 487 `RecoTrFastSeq` provides the necessary input to the run-by-run calibration and alignment,
 488 while the second best stage `RecoTrBestSeq` performs the remaining part of tracking
 489 reconstruction. The source code of algorithms and configuration of sequence can be found
 490 in Rec [1]. Since the tracking system is fully replaced by the new detectors, it requires a
 491 new reconstruction sequence with new dedicated algorithms:

```

492 RecoTrFastSeq
493   PrPixelTrackingFast           #VELO tracks finding
494   PatPV3D                       #Primary Vertex reconstruction
495   PrVeloUTFast                 #Upstream tracks finding
496   PrForwardTrackingFast        #Long (Forward) tracks finding
497   ForwardFitterAlgFast         #Kalman Filter Forward tracks
498 RecoTrBestSeq
499   PrForwardTrackingBest        #Long (Forward) tracks finding
500   PrHybridSeedingBest         #T-tracks finding
501   PrMatchNNBest               #Long (Match) tracks finding
502   PrLongLivedTrackingBest     #Downstream tracks finding
503   BestTrackCreatorSeq
504     TrackBestTrackCreator      #Kalman Filter and clone killing
505   TrackAddExtraInfoSeq
506     TrackAddNNGhostId         #Ghost Probability
  
```

507 The logic of the reconstruction is similar to already used for Run II. The reconstruction
 508 begins with the VELO tracking (`PrPixelTrackingFast`), where an internal simplified
 509 Kalman Filter is used. Those tracks are used to either reconstruct primary vertices (`PatPV`)
 510 or serve as seeds for the upstream tracking (`PrVeloUTFast`). In the recent implementation,
 511 at this stage the transverse momentum requirement is set to be greater than 300 MeV/c.
 512 The upstream candidates are then extended to SciFi detector, and the forward tracking is
 513 performed (`PrForwardTrackingFast`) with the transverse momentum threshold increased
 514 to 400 MeV/c. The last part of the fast `RecoTrFastSeq` stage is a Kalman Filter based
 515 track fit of all Forward candidates. The best stage mimics the HLT2 Run II sequence.
 516 First, the Forward tracks are found based on the VELO input (`PrForwardTrackingBest`).
 517 In contrast to the Run II sequence, already extended VELO tracks are reconsidered, since
 518 the flexibility written for Run II is not yet ported. A standalone T-track seeding is then
 519 performed (`PrHybridSeedingBest` [18]), which together with the VELO tracks provide
 520 the input the matching algorithm (`PrMatchNNBest` [19]). Finally, the downstream tracks
 521 are created using `PrLongLivedTrackingBest`. All dependencies among tracks are kept
 522 as shown in Fig. 1. The sequence finishes with the Kalman Filtering, where all duplicated
 523 tracks are removed.

524 In Run II, the optimised reconstruction algorithms allowed to loosen the p_T threshold
525 in the forward tracking from 1.2 GeV/c to 500 MeV/c in HLT1, significantly improving
526 the reconstruction efficiency of low momentum particles. The recent transverse mo-
527 mentum thresholds for the upgrade, 300 MeV/c for (**PrVeloUTFast**), and 400 MeV/c
528 (**PrForwardTrackingFast**) have been chosen due to improvements in the forward tracking.
529 These thresholds will however need to be optimised based on the timing and performance.
530 For the timing studies, two alternative transverse momentum threshold settings are
531 considered: a) intermediate cut: $p_T > 600$ MeV/c (**PrVeloUTFast**), $p_T > 800$ MeV/c
532 (**PrForwardTrackingFast**) b) hard cut: $p_T > 1.2$ GeV/c (**PrVeloUTFast**), $p_T > 1.4$ GeV/c
533 (**PrForwardTrackingFast**). Nevertheless, those thresholds are not yet fixed and need to
534 be carefully optimised based on both, timing and performance.

535 5.1.1 Developments since LHCb-PUB-2017-005 [20]

536 The performance reported in Ref. [20] has been obtained using the Run II framework.
537 Since then, a new framework has been developed which allows the efficient usage of
538 multithreading and parallelism paradigms. The two tracking stages, fast and best, have
539 been successfully ported to the new, functional framework.

540 In addition to this several changes has been made in the algorithms themselves. The
541 matching algorithm **PrMatchNNBest** has been reoptimised, where the main attention has
542 been paid to the Neural Net optimisation with a new set of variables. The new tuning
543 results with the speed up about 20% and reduction of the fake tracks from 26% to 20%
544 with minimal efficiency loss at the level of 0.5%.

545 In 2017 a new tuning for the downstream tracking has been performed where two
546 different multivariate techniques were employed. Firstly, the algorithm filters T tracks
547 using a bonsai Boosted Decision Tree with 11 dimensional discretised space resulting
548 in a rejection of fake seed tracks. Then the remaining T -track candidates are matched
549 with TT hits. Finally, the good track candidates are selected based on a neural network
550 decision. Overall signal efficiency improves by about $O(3 - 5\%)$, together with $O(3 - 5\%)$
551 improvement in fake track reduction. The improvements from **PatLongLivedTracking**)
552 can be ported to the upgrade tracking downstream algorithm **PrLongLivedTrackingBest**.

553 In addition, several changes have been made to the individual algorithms:

- 554 • **StoreVPClusters** and the nominal Velo Pixel tracking algorithm have been merged
555 into one algorithm, which was then been modified to be thread safe. This resulted in
556 a slight increase in the execution time. Following this, the memory usage of the this
557 algorithm, **PrPixelTrackingFast**, has been optimised by removing **KeyedObject**
558 and **KeyedContainer** for **VPClusters**. The structure used to store hits has been
559 changed to Structures of Arrays (SOA). These modifications result in 75% less
560 memory allocation and a timing reduction at the level of about 30% (with respect
561 to merged version).
- 562 • The matching algorithm **PrMatchNNBest** has been re-optimised, where the majority
563 of the attention has been paid to the Neural Net classifier optimisation with a new
564 set of variables. The new tuning gives a speed up at the level of about 20% and
565 reduction of the fake tracks from 26% to 20% with minimal efficiency loss at the
566 level of 0.5%. Further improvements are expected, including optimisation of track
567 fit model and further timing reduction.

568 • In 2017 a new tuning for the downstream tracking has been developed where two
 569 different multivariate techniques were employed. T-track candidates are selected
 570 using a bonsai Boosted Decision Tree (add Ref) which results in a significant rejection
 571 of fake seeds. The remaining T-track candidates are matched with TT hits and the
 572 good track candidates are selected based on a neural network decision. Overall signal
 573 efficiency improved by about $O(3 - 5\%)$, together with $O(3 - 5\%)$ improvement in
 574 fake track reduction. This development shows the potential direction of the future
 575 improvements for this particular type of tracking.

576 5.1.2 Ongoing developments

577 Preliminary throughput studies indicate that at least a factor of 6 speedup is still required
 578 to implement a sequence similar to that used in Run 2, however significant reductions to this
 579 factor can be made at some cost to the physics [21]. A critical part is the VELO tracking,
 580 which currently takes about 30% of the timing budget, and is mandatory to perform any
 581 physics measurement. Despite the merge of `StoreVPClusters` and the nominal VELO
 582 tracking algorithm, several additional improvements are under investigation:

- 583 • implementation of the `VPFilter`,
 584 which distinguishes tracks pointing from the primary and secondary vertices. It
 585 is another implementation of the $IP\chi^2$ requirement commonly used in the LHCb
 586 experiment and used for finding a well displaced tracks from the primary interactions.
 587 The `VPFilter` could serve as an alternative filter for selecting hits corresponding to
 588 only secondary particles in the detector, therefore reducing the time spent in the
 589 nominal VELO tracking.
- 590 • removing backwards tracks.
 591 The backwards tracks are needed for unbiased primary vertex reconstruction, however,
 592 physics analyses need only tracks associated to the particles passing through the
 593 detector in the forward direction. Removing the backward tracks reduces by $O(48\%)$
 594 the CPU requirements of the VELO tracking. The current studies show that
 595 this results in 20% poorer primary vertex resolution and 4% lower primary vertex
 596 efficiency.
- 597 • splitting and early breaking a pair creation for forward/backward tracks in the
 598 VELO tracking.
- 599 • using cellular automata in the VELO tracking.

600 Another part of the fast stage is the primary vertex reconstruction. The work fo-
 601 cuses on speeding up the code without significant efficiency and resolution degradation.
 602 The improvements consider changes in the seeding procedure, where the default three
 603 dimensional approach `PVSeed3DTool` has been changed to simplified two dimensional
 604 version `PVSeedTool`, with reoptimised settings. In addition to this, the default fitter
 605 `LSAdaptPV3DFitter` has been replaced by `AdaptivePV3DFitter`, with the corrected com-
 606 putation of primary vertex χ^2 as well as code speed up. The overall time improvement
 607 order of $O(65-70)\%$ is found, with negligible impact to the physics performance.

608 The main time consumer of both the fast and best reconstruction stages is a Kalman
 609 Filter, a linear quadratic estimator, which produces the final fitted tracks and their

610 associated covariance matrices. To achieve this goal several physics aspects have to
611 be considered such as multiple scattering or energy loss. There are many ongoing and
612 independent activities which have a potential of the significant time reduction without
613 performance loss. We briefly describe them:

- 614 • Cross Kalman [22],
615 which allows tracks to be processed in parallel. The goal is to perform calculations
616 using SIMD instructions while avoiding empty vector units. From a technical
617 point of view it is another implementation of `ITrackFitter`, developed as the
618 `TrackVectorFitter`.
- 619 • Parametrised Kalman,
620 the Kalman Filtering requires many track extrapolations from one detector layer
621 to the next, where the material and magnet field maps are needed. Possible time
622 reductions can be made by replacing the maps by parametrised layer to layer
623 predictions, which take into account the magnetic field intensity. Several different
624 parameterisations are used inside (VELO, UT, SciFi) and between (VELO-UT,
625 UT-SciFi) subdetectors. Preliminary studies show a factor of five speedup. This
626 algorithm has a potential to be used in the fast stage for fitting the Forward tracks.
- 627 • Simplified geometry [23],
628 the Kalman Filtering relies on the geometry used for the detector description, where
629 the number of volumes reduces from $O(10^6)$ to about 20 with the effective material.
630 Preliminary tests already indicate the speed by the factor ~ 10 -13 with respect to
631 the full geometry. The Simplified geometry has been used in Ref. [20], however work
632 is still ongoing and requires validation.

633 5.1.3 Future developments

634 The preliminary throughput studies show that the tight selection requirements are not
635 enough for running the recent tracking sequence at the 30 MHz bunch crossing rate. All
636 tracking algorithms need to be further revisited looking for the time improvements. The
637 main effort is focused on the speeding up the fast stage without significant performance
638 lost. As a well defined bottleneck, the possible improvements and/or compromises in
639 the VELO tracking are under extensive investigation. In addition, other part of the
640 fast stage are widely studies paying attention to the primary vertex finding and forward
641 reconstruction.

642 The effective memory usage requires a consistent use of SOA/AOS paradigms. The
643 data structures are optimally chosen for the specific algorithmic problem. Currently, the
644 data flow among tracking algorithms uses the AOS, the preliminary studies indicate no
645 visible profits from using the SOA. Therefore, changes in the data structure might require
646 reimplementations of particular algorithms. It is an important open topic for the future
647 discussions.

648 Another crucial topic is the clusters decoding in the Event Filter Farm. It has to be
649 understood whether the new detector's Readout Boards could perform the preliminary or
650 partial clusters sorting, which would result in the faster decoding.

5.2 Particle identification

5.2.1 RICH PID

The RICH reconstruction, as described in Section 2.2.1, has already been ported to the upgrade framework, and was very successfully used during 2017 data taking. As such the processing sequence already fully utilises the Function Framework, and the algorithms have been modified to make them re-entrant and thus thread safe.

Another aim during the modernisation process was to update the internal data structures used in the RICH, to pass information between the various sub-algorithms, to be more suitable for modern computing standards and in a format that promotes the use of techniques such as SIMD vectorisation. Utilisation of SIMD instructions is a critical aspect of the upgrade, as utilising these (increasingly) powerful instruction sets is the only way to fully exploit the full compute power of modern hardware. The developments in place for the 2017 Run II processing are only the first steps in this direction. Some explicit use of SIMD instructions were used, in the photon ray tracing, that lead to modest CPU improvements. Further work for Run III will focus on both extending this to the full reconstruction sequence, but also to more thoroughly using the SIMD instructions, and thus fully realising the expected gains from this area.

Finally, one aspect of the RICH reconstruction that has not been addressed is the final (persistent) event model, that saves the PID information for each track. This event model, will need to be heavily adapted for the upgrade. This work will follow in close harmony with the associated modernisation of the track objects.

5.2.2 Muon PID

The increase of the incident rate on the muon system will be tolerable up to the upgrade luminosity of $2 \times 10^{33} \text{cm}^{-2} \text{s}^{-1}$, in all stations apart from M1, which will be removed during LS2. Also, because of the particle flux expected on the innermost regions of M2 will be very high, an additional shielding will be installed around the beam-pipe behind the HCAL to reduce the occupancy in these regions. These will be the main hardware interventions foreseen at the upgrade, together with the installation of a new off-detector readout electronics compliant with full 40 MHz readout.

In this high luminosity scenario the muon identification algorithm must guarantee a high muon identification efficiency, while keeping the misidentification probability as low as possible. Due to the high hit occupancy expected at the upgrade running conditions, the `IsMuon` criterion plus a soft DLL cut produces an unacceptable increase of the misidentification probability of about a factor of two [24]. The two new variables `chi2Corr` and `muonMVA1` already available for the last year of Run II data taking allow to preserve the present identification versus misidentification performance.

Another muon identification algorithm has been developed in the context of the $K_S \rightarrow \mu^+ \mu^-$ physics analysis [25] to both improve the background rejection and increase the identification efficiency mainly for muons of low momenta. The tools developed for this algorithm are under study to be included in one or more new muon identification algorithms, `nIsMuon`, that could replace the actual `IsMuon` in Run III.

692 5.2.3 Calo PID

693 **SPD/PS removal** In Run III, the scintillating pad detector (SPD) and the preshower
694 (PS) of the current detector will be removed. The principal purpose of these components
695 in the current experiment is in the L0 trigger. The removal of the SPD/PS simplifies the
696 calorimeter system, with benefits for energy calibration and project costs. Nevertheless,
697 there are some consequences for the offline performance such as photon and electron
698 PID because the current estimators are using SPD/PS information. For instance, studies
699 reported in the LHCb PID Upgrade TDR show an absolute reduction of 10–15 % in photon
700 efficiency while electron PID is almost unchanged at high- p_T (above 10 GeV/c).

701 **Higher luminosity** The higher instantaneous luminosity in Run III and resulting
702 increased pile-up will impact on the energy resolution of the ECAL due to overlap of
703 neighbouring showers. To mitigate this effect, the current size of the clusters can be
704 reduced and two new shapes were investigated: 2×2 square and swiss-cross shapes. The
705 energy reconstruction with these new shapes mitigate to a large degree the effect of the
706 pile-up with respect to the present reconstruction, without significantly degrading the
707 energy resolution.

708 **Portability of current sequences** Reconstruction and PID sequences can already
709 be configured to ignore the SPD/PS information and use the alternative cluster shapes.
710 The CaloRecoConf and CaloPIDConf classes both use a boolean (`NoSpdPrs`) to choose
711 between current/upgrade geometry. The new shapes were implemented in the cluster
712 reconstruction through the options `ClusterEnergyMasks` and `ClusterPositionMasks` in
713 CaloRecoConf and will be set by default from the database. All PID algorithms, however,
714 needs to be adapted to these new shapes.

715 5.2.4 Global PID

716 For Run III a global PID sequence has not yet been defined. Different choices are possible
717 depending on the event model used. As far as the PID reconstruction sequences populate
718 the objects in the actual event model, the same set of combined likelihoods $\Delta \log \mathcal{L}_{comb}(X - \pi)$
719 as Run I and Run II is available. An improved version of the $\Delta \log \mathcal{L}_{comb}(X - \pi)$ variables
720 can be obtained using the improved performance of each single PID sub-detector as soon
721 as they are ready. The performance of such variables should inherit all those inbuilt in
722 the PID information of the muon, RICH, and calorimeter systems separately for Run
723 III. Another technically available choice is the use of the present definition of the `ProbNN`
724 variables which may make sense or not depending on the existence of the various input
725 variables. Finally the longer term solution of implementing new approaches equivalent to
726 the `ProbNN` variables, profiting of correlations among variables and of information from
727 non-PID systems, needs the definition of the new the event model.

728 6 Trigger

729 At its most general, the aim of a trigger is to reduce the amount of data recorded by a
730 detector to only that of interest for physics analysis. This can be achieved in two ways:
731 *reduction of rate* by separating events that contain interesting signals from those that do

732 not, and *reduction of size* by selecting the subset of the event that is useful for further
733 analysis. The present Run II trigger does both of these things, and the Run III trigger is
734 expected to do the same.

735 Reduction of rate is achieved through *selections*, where analysts choose events based on
736 a very broad range of discriminating criteria such as the invariant mass of a combination
737 of particles, the particle ID of daughter particles, vertex quality, track quality, *etc.* Two
738 types of selection are possible: *inclusive* selections save more than one decay type based
739 on general criteria, *e.g.*: ‘the decay of a B meson to any number of tracks’ and *exclusive*
740 selections where the full decay is completely specified, for example ‘the decay of a B meson
741 to two kaons and two muons’. In Run II the majority of the B signal rate is selected
742 inclusively using the topological triggers, while the majority of the D signal rate is selected
743 exclusively. In Run III both types of selection should be catered for.

744 Selections are defined by the analysts and as such we should endeavour to make
745 building these selections straightforward. In the present Run II trigger this is achieved
746 using LoKi functors.

747 Reduction of size is achieved through the *Turbo* paradigm, where analysts choose how
748 much of the event information they wish to persist. Potential objects to be persisted are:
749 the raw or derived event information from one or more subdetectors, the reconstructed
750 objects explicitly requested for an exclusive decay, partial selections of reconstructed
751 objects based on some criteria, *e.g.* ‘save all of the tracks in a cone surrounding this decay’,
752 *etc.*

753 This section describes the principal layout of the HLT1 and HLT2 sequences, meaning
754 the algorithms which bind together the different reconstruction stages and the algorithms
755 which are used to make a trigger decision and persist the trigger decision for analysis
756 usage.

757 Very few of these algorithms have been ported to the functional framework and no
758 work has been done on a potentially new event model from the Hlt side. In the following
759 sections we will layout the current design and later discuss the short comings of the
760 current design. This chapter should act as a guideline to prioritise and focus the software
761 development in the coming year.

762 **6.1 Selection framework**

763 The main task of the software trigger is to select signal events and candidates based on
764 the reconstructed objects. The online reconstruction is based on the algorithms described
765 in Section 2.

766 A requirement of HLT1 and HLT2 lines is to ensure that algorithms which produce
767 input to the decision making are run in the right order and are executed only once. The
768 layout of the decision sequences is different between HLT1 and HLT2. HLT1 selections
769 are based on partial event information, *e.g.* one or two track combinations only. HLT2
770 performs a full event reconstruction and full decay chains with many objects can be
771 reconstructed. Both are described in the following.

772 6.1.1 HLT1 selections

773 HLT1 lines are based on the streamer framework⁶. The streamer framework allows
774 reconstruction steps to be interleaved with selection cuts to only perform the necessary
775 operations. Every step of a trigger line is defined by a LoKi-functor which is passed if at
776 least one candidate passes the selection or reconstruction step.

777 As an example the code of the `Hlt1TrackMuon` streamer is given:

```
778 TrackCandidates
779 >> ((TrPT > %(PreFitPT)s * MeV) & (TrP > %(PreFitP)s * MeV))
780 >> FitTrack
781 >> ((TrPT > %(PT)s * MeV ) & (TrP > %(P)s * MeV ))
782 >> ((TrCHI2PDOF < %(TrChi2)s) & (Tr_HLTMIPCHI2('PV3D') > %(IPChi2)s ))
783 >> IsMuon
784 >> SINK('Hlt1%(name)sDecision')
785 >> ~TC_EMPTY
```

786 The input to the line are long tracks coming from the `TrackCandidates` functor. To
787 reduce the number of tracks to fit, a preselection on the momentum is performed. Track
788 quality and impact parameter requirements are placed after the track fit. Finally, the
789 trigger candidate has to be identified as a muon. The `SINK` functor saves the decision of
790 the line.

791 The streamer framework itself does not guarantee that the reconstruction algorithms
792 which provide the input to selections are run. If a functor needs external input, this
793 has to be specified separately, *e.g.* the `Tr_HLTMIPCHI2('PV3D')` functor requires that the
794 primary vertex reconstruction is executed.

795 Therefore the the layout of an `Hlt1Line` looks like this:

```
796 Hlt1Line('TrackMuon',
797         prescale = 0..1,
798         postscale = 0..1,
799         priority = 0..,
800         LODU = 'LOMuon|LODiMuon',
801         algos = [ Hlt1GECUnit('Loose'),
802                 PV3D('Hlt1'),
803                 trackingAlgos,
804                 streamer ]
805 )
```

806 Additional selections which can be set are prescales, postscales, ODIN, L0 requirements
807 and global event cuts. The latter is defined in the algorithm sequence.

808 6.1.2 HLT2 selections

809 The information available to HLT2 lines changed drastically between Run I and Run II.
810 While in Run I particle identification could only be run for selected lines after a further
811 reduction of events, in Run II basically the full offline reconstruction is run in HLT2. This
812 means that in Run II every line specifies the full offline reconstruction as input while in

⁶A more detailed description of the HLT1 streamer framework is given in Reference [26].

813 Run I different lines could have different levels of reconstruction, *e.g.* with or without
814 particle identification to fulfil the timing requirements.

815 Most HLT2 selections combine basic particle candidates to composite particle candi-
816 dates, referred to as *combinatorics* in the next section.⁷ The input to most HLT2 lines are
817 basic `Particle`s. A basic `Particle` is built out of a `LHCb::ProtoParticle`, in form of a
818 pointer, which holds the full reconstructed information and an assigned particle hypotheses,
819 *e.g.* the kaon, pion, electron, muon or proton hypotheses. Different `Particles` can be
820 built out of the same `ProtoParticle`. The `ProtoParticle` holds pointers to different
821 reconstructed objects like in the case of a charged particle a track and the associated
822 particle identification objects.

823 As the HLT1 lines, HLT2 lines have to declare manually their inputs to guarantee that
824 the reconstruction sequence provides all necessary information; *e.g.* a common pitfall in
825 HLT2 lines is that impact parameter cuts which require the existence of the primary vertex
826 reconstruction do not declare the primary vertex reconstruction as an input, eventually
827 leading to a loss of these events or depending on the luck that another line provided the PV
828 reconstruction. Another pitfall mainly in Run I was that different paths of reconstruction
829 existed. So a line which used PID cuts had to specify different dependencies than a line
830 which did not use PID cuts.

831 6.1.3 Combinatorics

832 Finding “good” multibody combinations of particles is generically referred to as “combi-
833 natorics”. In the current trigger then “good” is rather analysis-dependent, but typical
834 criteria are that the charged particle tracks form a vertex with small χ^2 , and that this
835 vertex is displaced from the PVs.

836 The relevant algorithms in the old framework are `CombineParticles`
837 and `DaVinci::N{3,4,5,6,7,8}BodyDecays`. These take several containers of
838 `LHCb::Particle` objects (*e.g.* kaons, muons, ...) as input, and produce a new
839 container of `LHCb::Particle` as output, applying cuts at several stages internally. The
840 vertex fit is performed by a tool, typically `LoKi::VertexFitter`. There are three types
841 of selection applied by these algorithms:

- 842 • `DaughtersCuts` that remove particles in the input containers from consideration,
- 843 • `CombinationCut` that act on n -body tuples of particles (before the vertex fit), and
- 844 • `MotherCut` that act on n -body composite particles (after the vertex fit).

845 The `DaVinci::N{3,4,5,6,7,8}BodyDecays` algorithms add extra versions of the
846 `CombinationCut` called `CombinationCut12`, `CombinationCut123` *etc.* that are applied
847 to 2-body, 3-body *etc.* tuples of particles and allow bad combinations to be rejected more
848 efficiently. Typical examples of cuts that are applied at each stage are:

- 849 • `DaughtersCuts` displacement from PVs (χ_{IP}^2 - `BPVIPCHI2`), PID information (`PIDK`),
850 p_T thresholds (`PT`)
- 851 • `CombinationCut{,12,123,...}` pairwise distance between tracks (χ_{DOCA}^2 -
852 `ADOCACHI2`), vector and/or scalar sum of child transverse momenta (`APT`, `ASUMPT`),
853 pre-vertex-fit parent mass (`AM`)

⁷Examples of HLT2 lines can be found in `gitlab Hlt/Hlt2Lines`.

854 • `MotherCut` vertex fit quality ($\chi_{\text{vtx}}^2 - \text{CHI2VX}$), post-vertex-fit parent mass (`M`)

855 Note that the first of these, the `DaughtersCuts`, could be implemented by placing ap-
856 propriate filtering algorithms in front of `CombineParticles`, and the `MotherCut` could
857 be implemented by attaching a filter to the output, but the `CombinationCut` is tightly
858 integrated into the algorithm.

859 In Run II there is no protection against running the vertex fit multiple times on the
860 same set of n input particles in different selections. Additionally, because the inputs of
861 these algorithms are `LHCb::Particle` not `LHCb::Track`, the same set of particles may be
862 fitted several times under different mass hypotheses (pion, kaon, *etc.*), even though the
863 assigned mass has no, or negligible, impact on the fit. This is mitigated by the use of PID
864 information in `DaughtersCuts` in the Run II trigger, but it may not be possible to run
865 the PID reconstruction before every trigger line.

866 6.1.4 Looking forward

867 Running HLT1 at 30 MHz will be challenging. Assuming the current budget of 1000
868 farm nodes, this means that every farm node has to process 30k events per second. An
869 HLT1 framework which adapts the functional framework and runs together with a multi-
870 threaded scheduler needs to be developed. The concepts of the HLT1 streamer model
871 map well onto the functional framework, albeit the implementation will need a lot of
872 changes, *e.g.* classes like `HltBaseAlg` and `HltSelection` can be seen as a direct ancestor of
873 `Gaudi::Functional`. To profit from newer architectures it should act on containers and not
874 single objects, *e.g.* the streamer framework heavily relies on the `tracksFromTrack(const`
875 `LHCb& Track track, std::vector<LHCb::Track> output)` interface. This interface
876 inherently makes horizontal vectorisation more complicated⁸.

877 For the upgrade we have to maintain the possibility that different HLT2 lines can
878 specify different reconstructions. It will likely be the case that the same reconstruction will
879 be the basis for many trigger lines. The functional framework which focuses on properly
880 defining inputs and outputs removes the boilerplate in the python configuration. The
881 input and output matching is moved to the scheduler of Gaudi and will guarantee the
882 existence of the right inputs and outputs. This will help to simplify the writing of HLT2
883 and potentially HLT1 lines and will make them more closely resemble what is being done
884 in *Stripping* and user-job selections.

885 It is an open question whether or not in Run III it will be more computationally
886 efficient to keep the Run II model, or to replace it with an “up front” combinatorics engine
887 that finds all 2-track, 3-track, ... combinations that form a good vertex and provides these
888 as inputs to the trigger selections. It is clear that with the higher luminosities and higher
889 track multiplicities of Run III the combinatoric timing will be more difficult to control
890 than in Run II. Additionally, in Run III it might be more efficient to seed HLT2 selections
891 from HLT1 candidates, rather than starting from scratch and matching afterwards.

892 Another idea for multi-body combinations is the following: if multi-body particle
893 combinations are formed up-front without reference to specific mass hypotheses, more
894 efficient clustering algorithms can be used than in the current trigger. For a simple
895 illustration of this, assume that the selection requirements are expressed as a “seed”
896 requirement that one particle in the combination must satisfy, and a second requirement

⁸Nevertheless, benchmarking the throughput should drive the design process

897 that every pair of particles must pass. In this case, the search for the 3rd and subsequent
898 particles in the combination must only cover a small subset of particles in the event that
899 are known to satisfy the pairwise requirement.

900 **6.2 Persistency**

901 The meaning of persistency is two fold in the Run II trigger, the first is the persistency of
902 trigger decisions and trigger objects used in offline reconstructed data, the second is the
903 persistency of trigger objects in the Turbo stream where no further offline reconstruction
904 is performed.

905 **6.2.1 Persistency of trigger decisions**

906 It is important to know which trigger lines selected an event and which trigger objects lead
907 to a positive trigger decision in offline analysis. Both types of information are persisted at
908 the end of every event. The trigger decisions are saved in the `HltDecReports` and the
909 `HltSelReports`.

910 For every trigger line present a `HltDecReport` is persisted. A `HltDecReport` are two
911 16-bits mask where the first is the identifier and the second contains amongst other the
912 information if the given trigger line selected the event, how many trigger candidates the
913 line created and also basic information in which selection step the trigger line failed. The
914 `HltDecReport` are written by the `HltDecReportsWriter` and can be decoded from the
915 raw event by the `HltDecReportsDecoder`.

916 A `HltSelReport` contains the necessary information to match a particle candidate
917 used in the trigger to a particle candidate created in the offline processing. The particle
918 candidate can be a composite object or basic particle, like e.g. a pion or a muon
919 candidate. The matching itself is based on `LHCbIDs` of the primitive reconstructed objects,
920 like tracks in the tracking system, calorimeter cluster or muon tracks. For that the
921 `HltSelReportsMaker` and the `HltReportConvertTool` extract the `LHCbIDs` from the
922 basic objects and save it in a structure which corresponds to the structure of the trigger
923 candidate, i.e. the `HltSelReport` allows to decode later of which particle candidates a
924 composite object was made of. In addition to the `LHCbIDs` some basic information like
925 the momentum or the fit quality of a reconstructed track are persisted. The reports are
926 then written to the raw event by the `HltSelReportsWriter`.

927 **6.2.2 Turbo persistency**

928 Events in which at least one Turbo line fired are sent to the `TURBO` stream, where
929 most of the raw information is discarded. In 2015 and 2016, candidates firing Turbo
930 lines were persisted in the previously described `HltSelReports`, which were extended to
931 accommodate the additional information required to ‘resurrect’ the full `Particle` objects,
932 from the reports, for use offline. The conversion from information in the `HltSelReports`
933 to analysis objects, like `Track`, `CaloCluster`, and `Particle`, was performed by the `TESLA`
934 application.

935 In 2016, the `PersistReco` flag was made available on a per-line basis. For events with
936 firing Turbo lines that have the `PersistReco` flag enabled, the entire HLT2 reconstruction
937 is persisted, along with the trigger candidate as before. Rather than attempting to store
938 the entire reconstruction in the `HltSelReports`, the packed reconstruction is serialised in

939 to the as-of-then unused `DstData` raw bank. This raw bank is propagated through Tesla,
940 and is de-serialised and unpacked in user analysis jobs. The packing is performed by
941 the standard packing algorithms (*e.g.* `PackTrack` and `PackParticlesAndVertices`), and
942 the (de-)serialisation is done by the `HltPackedDataWriter` and `HltPackedDataDecoder`
943 algorithms.

944 The introduction of `PersistReco` meant the existence of two persistence strategies.
945 In an attempt to unify these, the persistence of Turbo candidates was migrated to the
946 `PersistReco` model in 2017: candidates that fire any Turbo HLT2 line are packed and
947 persisted in the `DstData` raw bank. This has two advantages:

- 948 1. The `HltSelReports` are no longer extended beyond their original purpose, and
949 the complex (de-)serialisation code can be removed. It is then no longer possible
950 for Turbo candidates to interfere with the TIS/TOS mechanism, which uses the
951 `HltSelReports` (such interference caused a bug which required a re-stripping of
952 2015 and 2016 data), and the number of Turbo-specific algorithms is reduced.
- 953 2. Turbo candidates are treated in the same way as the rest of the HLT2 reconstruction.
954 This allows for fine-grained per-line control as to what parts of the reconstruction
955 are saved (*e.g.* only tracks which form a good vertex with the trigger candidate),
956 and prevents a class of problems caused by Turbo candidate tracks not being
957 pointer-equivalent to `PersistReco` tracks.

958 In principle, Tesla then only needs to convert from the online `.mdf` format to a DST,
959 but in practice Tesla implements streaming in a similar manner to the Stripping. This
960 loosely groups together lines by physics category and saves each group in separate output
961 files, with the intention of reducing the number of files individual analysts have to process.

962 Both the online implementation of the Turbo persistence model and the of-
963 fline implementation of Tesla make extensive use of the μ DST cloning framework
964 (which gives in various `MicroDST*` packages under the `MicroDST` hat in `Phys`). At
965 the highest level, the framework consists of algorithms which can each clone some
966 `KeyedContainer`, from `/Event/Some/Location` to `/Event/<prefix>/Some/Location`,
967 using a cloner tool. The same algorithm may also use other cloner tools to clone the
968 ‘dependencies’ of each `KeyedObject` in a similar manner. For example, `Particle` contain-
969 ers can be cloned with the `ParticleCloner` algorithm, which will also clone associated
970 `Vertex` and `ProtoParticle` objects with implementations of the `ICloneVertex` and
971 `ICloneProtoParticle` tools.

972 In HLT2, the cloner framework is used to copy the set of `Particle` objects created by
973 firing Turbo lines, as well as subsets of the reconstruction requested by lines, from their
974 original locations to those under the `/Event/Turbo` prefix. All objects under this prefix are
975 then packed and persisted to the `DstData` bank. The introduction of the cloner framework
976 into HLT2 in 2017 allowed for the persistence of only the parts of the reconstruction
977 relevant to offline analysis, as opposed to 2016 when only the whole, original containers
978 could be persisted.

979 In Tesla, the cloners are used for streaming, as in the Stripping. Each HLT2 line is
980 assigned to a stream, and then all of the locations requested by that line are copied to the
981 respective stream for each event in which the line fired. The list of locations requested by
982 a line, which includes the location of the `Particle` objects used to the make the trigger
983 decision, is defined by the TCK. The mapping from line name to output stream is defined
984 in the Tesla configuration.

985 6.2.3 Tesla

986 The TESLA application converts from the `.mdf` format output by HLT2 into something
987 which is easily analysable in DAVINCI. Ignoring streaming, in 2017 this means:

- 988 1. Decoding the `DstData` bank and persisting the resulting packed containers (so that
989 user jobs don't need to decode the bank themselves);
- 990 2. Decoding the HLT1 and HLT2 `HltSelReports`, removing Turbo reports from the
991 latter, and persisting both. The `RecSummary` is encoded in the `HltSelReports` in
992 HLT2, so this is decoded in TESLA and the resulting `Rec/Summary` location is also
993 persisted.
- 994 3. Juggling the raw event and persisting the resulting locations (most raw banks are
995 removed by the `TURBO` stream writer in HLT2).

996 In DAVINCI user jobs, the packed containers from TESLA are unpacked, and symbolic
997 links are created from the HLT2 reconstruction output locations to those of BRUNEL,
998 such that most standard analysis tools do not need to be configured specifically to analyse
999 Turbo data (as, for example, they expect `Track` objects to be in `Rec/Track/Best` rather
1000 than `Track/Best/Long`).

1001 For simulated events, TESLA also creates relations tables for `ProtoParticle` \leftrightarrow
1002 `MCParticle` and `CaloCluster` \leftrightarrow `MCParticle` matching. For μ DST output, the list of
1003 `MCParticle` and `MCVertex` objects are filtered, based on the simulated signal process and
1004 the MC objects that can be associated to the HLT2 reconstruction.

1005 Streaming in TESLA is implemented using the μ DST cloner framework, whereby
1006 HLT2 lines are grouped into streams, and each stream is an output file containing only
1007 the information required by the particular HLT2 lines.

1008 6.2.4 Looking forward

1009 The size of the `HltDecReports` could be reduced if one would save the `HltDecReport` only
1010 for trigger lines which fired in an event. It would imply the removal of the information
1011 in which selection step a trigger line failed. However, this information is hardly used
1012 offline and the information is anyhow biased as it is only available in events which got
1013 selected by another trigger line. Given that we expect more than a thousand trigger lines
1014 in the upgrade this might be a sizeable reduction. The information is useful in the online
1015 monitoring of the Hlt and can be persisted in monitoring histograms.

1016 The `HltSelReports` store reconstructed information in a specialised format that is
1017 incompatible with standard analysis tools: one cannot simply retrieve particle momentum
1018 from the `HltSelReports`, for example. Instead, it seems desirable to save the information
1019 about trigger candidates in the default event format to benefit from developments there.
1020 A first step towards this was made in 2017 and is described in the the next section about
1021 Turbo persistency.

1022 Packing, used both in HLT2 and TESLA, is expected to be play an important role in
1023 the upgrade, as it can compress the data using knowledge about the detector noise and its
1024 dynamic range. For example, a `double` may not be required for storage if a measurement
1025 is not very precise, but it is useful to use when performing computations in memory. The
1026 cloner framework, on the other hand, can be considered as an implementation detail,

1027 existing because GAUDI can only persist entire containers of objects. As we often require
1028 only certain objects within containers to be persisted, *e.g.* only the information requested
1029 by Turbo lines, we must first clone that information to new containers. This requires time,
1030 to perform the copy operations, and consumes additional memory, that required to hold
1031 the cloned objects. There is no current plan for replacing the cloner framework, although
1032 the possibility of alternatives should be investigated.

1033 Given that the full raw event can only be saved in rare cases it has to be ensured that
1034 the possibility to perform detector calibrations is available, *e.g.* one could imagine to refit
1035 tracks with a different alignment or apply a better calibration of the calorimeter offline.
1036 Especially, the calorimeter calibration needs more data than can be collected in one fill,
1037 making it difficult to provide the best calibration before HLT2 runs.

1038 A more invasive idea would be to only save the LHCbIDs and associated detector
1039 response for selected candidates and discard all reconstructed information at the end of
1040 HLT2. The information then could be recreated offline rerunning the same algorithms as
1041 done online. This will be an optimisation between offline storage and CPU resources and
1042 it needs to be ensured that enough information is saved to recreate the full information.

1043 Currently, data from the pit is not compressed before being sent offline. The `.mdf`
1044 format supports compression of raw information within events, and the `DstData` bank
1045 used for writing Turbo information is compressed by the `HltPackedDataWriter`, but
1046 further gains may be possible simply by compressing whole `.mdf` files. This is illustrated
1047 in Fig. 2. Using the `xz` compression algorithm, it has been seen that savings of 10–15 %
1048 can be made with respect to the current strategy in 2017.

1049 It is a matter of discussion how much of the work done in TESLA could be moved
1050 into MOORE. For example, MOORE already streams events into *e.g.* the FULL and TURBO
1051 streams, and preserves only certain information in certain streams. Streaming into TURBO
1052 could become more granular to prevent the need for streaming in TESLA. In addition, it
1053 would be nice to avoid the encoding of packed containers in MOORE, which is followed
1054 by decoding in TESLA, and rather just write and read packed containers directly. The
1055 inability to do this today is a feature of the `.mdf` format.

1056 7 Conclusion

1057 This note has outlined the current state of the baseline trigger and reconstruction strategy
1058 as of the end of 2017. The next steps, to be implemented in future documents, is a
1059 performance benchmark of the implemented algorithms, and studies of the HLT selections.

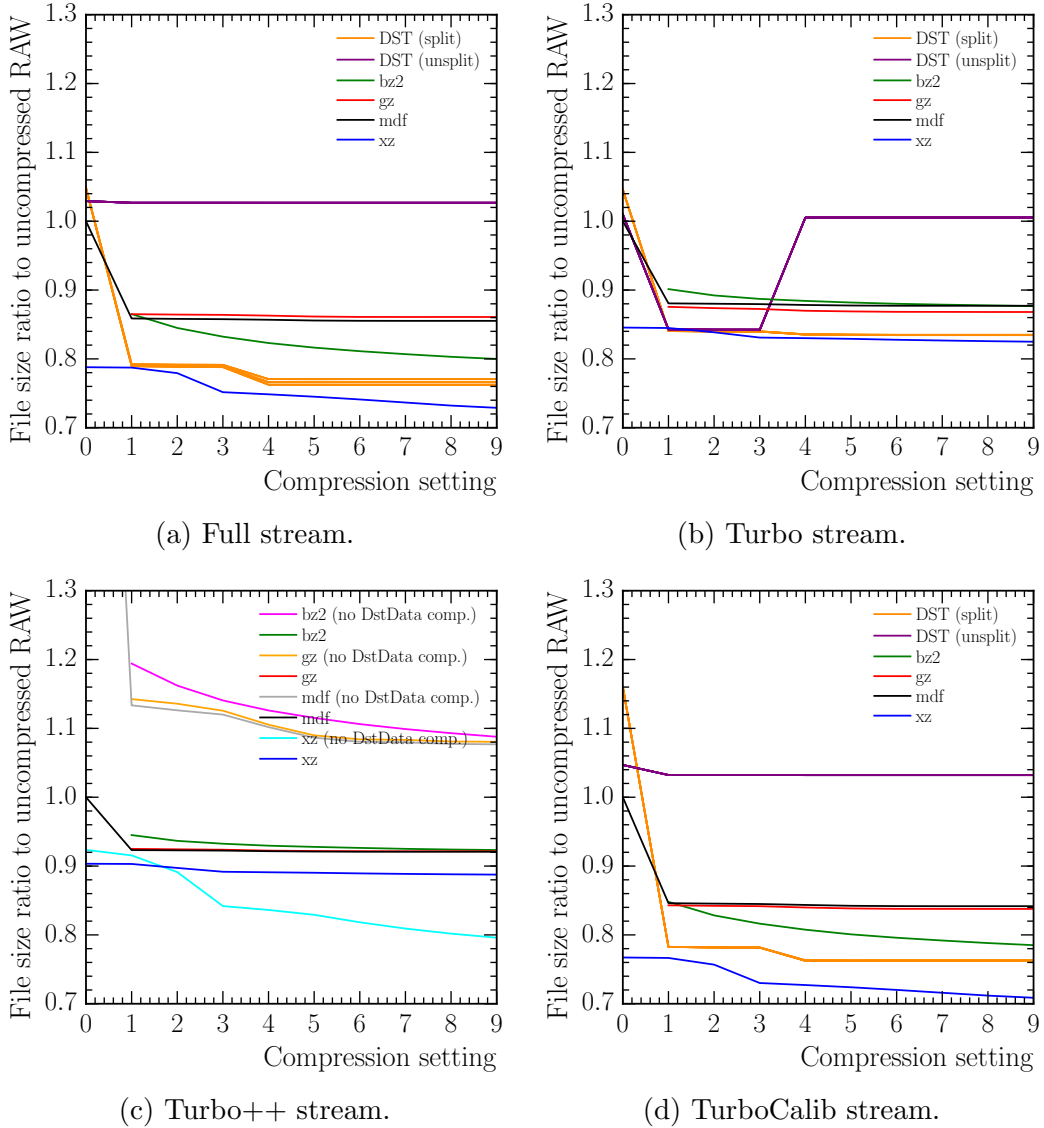


Figure 2: Comparison of compression ratios obtained by a variety of compression algorithms on the output of the Run II HLT2. Figure 2a shows the performance on the full stream, which contains the full raw event information and Run-I-like `H1tSelReports`, Fig. 2b is evaluated on Turbo data that includes Turbo `H1tSelReports` and Fig. 2c takes as input the subset of Turbo data that have the full reconstructed event information persisted in the `DstData` raw bank (Turbo++). Figure 2d is evaluated on the TurboCalib stream, which includes both the full raw event information and Turbo `H1tSelReports`. In Fig. 2c the curves labelled “no `DstData` comp.” show the results when the internal compression of the `DstData` raw bank is disabled. The DST configuration uses ROOT’s LZMA compression, and multiple DST curves correspond to different setting for the ROOT basket and buffer sizes.

References

- 1060
- 1061 [1] LHCb collaboration, *Rec gitlab repository*, <https://gitlab.cern.ch/lhcb/Rec>.
- 1062 [2] O. Callot, *FastVelo, a fast and efficient pattern recognition package for the Velo*,
1063 Tech. Rep. LHCb-PUB-2011-001. CERN-LHCb-PUB-2011-001, CERN, Geneva, Jan,
1064 2011. LHCb.
- 1065 [3] O. Callot and M. Schiller, *PatSeeding: A Standalone Track Reconstruction Algorithm*,
1066 Tech. Rep. LHCb-2008-042. CERN-LHCb-2008-042, CERN, Geneva, Aug, 2008.
- 1067 [4] E. E. Bowen, B. Storaci, and M. Tresch, *VeloTT tracking for LHCb Run II*, Tech. Rep.
1068 LHCb-PUB-2015-024. CERN-LHCb-PUB-2015-024. LHCb-INT-2014-040, CERN,
1069 Geneva, Apr, 2016.
- 1070 [5] O. Callot and S. Hansmann-Menzemer, *The Forward Tracking: Algorithm and*
1071 *Performance Studies*, Tech. Rep. LHCb-2007-015. CERN-LHCb-2007-015, CERN,
1072 Geneva, May, 2007.
- 1073 [6] M. Needham and J. Van Tilburg, *Performance of the track matching*, Tech. Rep.
1074 LHCb-2007-020. CERN-LHCb-2007-020, CERN, Geneva, Mar, 2007.
- 1075 [7] M. Needham, *Performance of the Track Matching*, Tech. Rep. LHCb-2007-129.
1076 CERN-LHCb-2007-129, CERN, Geneva, Oct, 2007.
- 1077 [8] A. Davis, M. De Cian, A. M. Dendek, and T. Szumlak, *PatLongLivedTracking:*
1078 *A tracking algorithm for the reconstruction of the daughters of long-lived particles*
1079 *in LHCb*, Tech. Rep. LHCb-PUB-2017-001. CERN-LHCb-PUB-2017-001, CERN,
1080 Geneva, Jan, 2017.
- 1081 [9] M. De Cian, S. Farry, P. Seyfert, and S. Stahl, *Fast neural-net based fake track*
1082 *rejection*, Tech. Rep. LHCb-PUB-2017-011. CERN-LHCb-PUB-2017-011, CERN,
1083 Geneva, Mar, 2017.
- 1084 [10] M. Kucharczyk, P. Morawski, and M. Witek, *Primary Vertex Reconstruction at LHCb*,
1085 Tech. Rep. LHCb-PUB-2014-044. CERN-LHCb-PUB-2014-044, CERN, Geneva, Sep,
1086 2014.
- 1087 [11] A. Dziurda, V. V. Gligorov, and M. Witek, *Primary Vertex Reconstruction for Run II*
1088 *of data taking*, Tech. Rep. LHCb-INT-2016-034. CERN-LHCb-INT-2016-034, CERN,
1089 Geneva, Jul, 2016.
- 1090 [12] B. Storaci, *Optimization of the LHCb track reconstruction*, J. Phys. : Conf. Ser. **664**
1091 (2015) 072047. 6 p.
- 1092 [13] LHCb collaboration, *Brunel gitlab repository*, <https://gitlab.cern.ch/lhcb/Brunel>.
- 1093 [14] A. A. Alves Jr. *et al.*, *Performance of the LHCb muon system*, JINST **8** (2013)
1094 P02022, arXiv:1211.1346.

- 1095 [15] G. Lanfranchi *et al.*, *The Muon Identification Procedure of the LHCb Experiment*
1096 *for the First Data*, Tech. Rep. LHCb-PUB-2009-013. CERN-LHCb-PUB-2009-013,
1097 CERN, Geneva, Aug, 2009.
- 1098 [16] LHCb collaboration, R. Aaij *et al.*, *LHCb detector performance*, Int. J. Mod. Phys.
1099 **A30** (2015) 1530022, [arXiv:1412.6352](https://arxiv.org/abs/1412.6352).
- 1100 [17] LHCb collaboration, *LHCb Upgrade Software and Computing TDR*, CERN-LHCC-
1101 2018. in preparation.
- 1102 [18] R. Quagliani, Y. S. Amhis, P. Billoir, and F. Polci, *The Hybrid Seeding algorithm*
1103 *for a scintillating fibre tracker at LHCb upgrade: description and performance*, Tech.
1104 Rep. LHCb-PUB-2017-018. CERN-LHCb-PUB-2017-018, CERN, Geneva, May, 2017.
- 1105 [19] S. Esen and M. De Cian, *A Track Matching Algorithm for the LHCb upgrade*, Tech.
1106 Rep. LHCb-PUB-2016-027. CERN-LHCb-PUB-2016-027, CERN, Geneva, Dec, 2016.
- 1107 [20] R. Aaij *et al.*, *Upgrade trigger: Biannual performance update*, Tech. Rep. LHCb-
1108 PUB-2017-005. CERN-LHCb-PUB-2017-005, CERN, Geneva, Feb, 2017.
- 1109 [21] M. De Cian *et al.*, *Status of HLT1 sequence and path towards 30 MHz*, Tech. Rep.
1110 LHCb-PUB-2018-003. CERN-LHCb-PUB-2018-003, CERN, Geneva, Mar, 2018.
- 1111 [22] D. H. Cámpora Pérez and O. Awile, *An efficient low-rank Kalman filter for modern*
1112 *SIMD architectures*, submitted to Concurrency and Computation: Practice and
1113 Experience.
- 1114 [23] B. Couturier and T. Szumlak, *Simplified Detector Description for LHCb Upgrade*,
1115 Tech. Rep. LHCb-PUB-2017-003. CERN-LHCb-PUB-2017-003, CERN, Geneva, Jan,
1116 2017.
- 1117 [24] LHCb collaboration, *LHCb PID Upgrade Technical Design Report*, CERN-LHCC-
1118 2013-022. LHCb-TDR-014.
- 1119 [25] LHCb collaboration, R. Aaij *et al.*, *Improved limit on the branching fraction of the*
1120 *rare decay $K_S^0 \rightarrow \mu\mu$* , Eur. Phys. J. **C77** (2017) 678, [arXiv:1706.00758](https://arxiv.org/abs/1706.00758).
- 1121 [26] R. Aaij, G. Raven, and M. Merk, *Triggering on CP Violation: Real-Time Selection*
1122 *and Reconstruction of $B_s \rightarrow J/\psi\phi$ decays*, Jan, 2015. Presented 07 May 2015.